Room Temperature Precipitation in Dilute Al-Li Alloys

János Lendvai*, Hans-Joachim Gudladt, Wilfried Wunderlich, and Volkmar Gerold

(Max-Planck-Institut für Metallforschung, Institut für Werkstoffwissenschaft, Stuttgart, und Institut für Metallkunde der Universität Stuttgart, Seestraße 92, D-7000 Stuttgart 1)

Dedicated to Professor Dr. Theodor Heumann on the occasion of his 75th birthday

In Al-Li alloys aged at 433 or 473 K for 10 to 48 h further precipitation was observed in course of room temperature (RT) storage subsequent to the artifical ageing treatment. This post-ageing phenomenon was investigated by electron microscopy and by calorimetric measurements. The nucleation and growth of new particles during the RT ageing leads to a bimodal distribution of precipitates with strongly differing mean particle sizes. On the basis of these results conclusions could be drawn as to the characteristic features of the precipitation process at or near RT. The question whether in Al-Li alloys on the basis of structural or compositional differences GP zones have to be distinguished from δ' precipitates will be also discussed.

Ausscheidungsvorgänge bei Raumtemperatur in Al-Li Legierungen

In Al-Li-Legierungen, die bei 433 oder 473 K jeweils 10 bis 48 h ausgelagert worden sind, wurde weitere Ausscheidungsbildung während der Raumtemperaturauslagerung beobachtet, die nach der Warmauslagerung stattgefunden hatte. Das Phänomen dieses Teilchenwachstums während der Nachauslagerung konnte sowohl mit Hilfe elektronenmikroskopischer als auch kalorimetrischer Messungen beobachtet werden. Die Bildung und das Wachstum der Teilchen während der RT-Auslagerung führt zu einer bimodalen Verteilung mit stark differierendem mittleren Teilchendurchmesser. Aus diesen Ergebnissen können Rückschlüsse auf die Bildungsprozesse der Teilchen bei Raumtemperatur gezogen werden. Die Frage, inwieweit in Al-Li-Legierungen die neugebildeten Teilchen aufgrund der Struktur und der Zusammensetzung als GP-Zonen aufgefaßt werden können, soll ebenfalls diskutiert werden.

1 Introduction

The strengthening of Al-Li alloys is due to the highly disperse precipitation of coherent, spherical, $L1_2$ ordered δ' (Al_3Li) precipitates. The formation and growth of δ' particles has been the subject of many investigations, the most important results have been reviewed several times and summarized e.g.[1)2)3)]. The interactions between dislocations and δ' precipitates and the fundamental strengthening mechanisms in binary high purity alloys have been extensively studied in recent years with single crystals[4)5)] as well as with polycrystals[6)7)].

Fatigue tests on single crystals oriented for single slip revealed planar slip in the case of underaged as well as of peak-aged specimens which has a strong influence on the fatigue behaviour of this alloy[8)]. The planar slip is caused by dislocation shearing of the ordered δ' precipitates which grow typically 20 to 40 nm in diameter during the ageing treatment. It is well established that planar slip occurs also in other alloys containing $L1_2$ ordered particles, especially in γ'-hardened Ni alloys[9)10)].

In addition to precipitation-hardened alloys containing ordered particles, planar slip has also been observed in solid solution hardened alloys like Cu-Mn[11)] or in Ni_3Fe[12)] having a high stacking fault energy (SFE). It was concluded[12)] that in these and other cases mostly short range ordering (SRO) leads to planar slip and, therefore, the influence of the SFE on the planar slip should be less important.

The observations described above are very important for the present case because planar slip was also found in Al-Li single crystals aged for 5 days at room temperature (RT) after homogenization followed by water-quenching. In these specimens the δ' particles which are formed during ageing at 433 or 473 K were not observed. Therefore there must be other reasons for the occurrence of planar slip.

Differential scanning calorimetric (DSC) measurements revealed that the dissolution of the δ' precipitates formed on ageing between 433 and 493 K takes place in an endothermal reaction with a peak temperature about 80 K higher than the ageing temperature[13)] to [15)]. In the present work another endothermal reaction has been detected in the DSC curves of artificially aged Al-Li samples far below the temperature of the endotherm process corresponding to the dissolution of the δ' particles which had been formed during the artificial ageing treatment. It was assumed that this low temperature endotherm reflects either the dissolution of precipitates or the disordering of short range ordered clusters formed during the RT storage subsequent to the artificial ageing treatment. This post-ageing phenomenon was investigated in the present work by DSC and electron microscopy (TEM and HREM) investigations. From the results conclusions can be drawn concerning the precipitation processes in the temperature range around RT. The question whether in Al-Li alloys GP zones have to be distinguished from δ' precipitates on the basis of structural or compositional differences will be also discussed.

2 Experimentals

The investigations were carried out on high purity binary Al-Li single crystals prepared of 6N purity Al and 4N purity Li by the Bridgman technique. The results described in this paper were obtained primarily on crystals containing 8.5 ± 0.1 at.% Li, but results of DSC measurements carried out on specimens of other compositions are also included (see Fig. 3 and Table 1). The composition of each specimen has been determined by atomic absorption spectroscopic

* On leave from the Institute for General Physics, Eötvös University, Budapest, Hungary.

analysis and/or by density measurement after the single crystal preparation.

The samples were solution heat treated in a salt bath at 838 K for 30 min, water-quenched and naturally aged at RT for about 4 days. The artificial ageing treatments were carried out in thermostated oil baths. Disk-shaped samples of 0.6 and 0.2 mm thickness were spark-cut for the DSC and TEM investigations, respectively.

DSC measurements have been performed by using a Perkin-Elmer DSC-2 calorimeter at 80 K · min^{-1} heating rate on samples of about 20 mg. The DSC runs started at 270 K. High purity aluminium of approximately the same mass as that of the sample was used as the reference. All data were stored by a personal computer which was connected to the DSC equipment. Subsequently, a baseline was subtracted from the data. The baseline was obtained by replacing the specimen in the calorimeter by high purity aluminium of about the same mass and repeating the run under exactly the same conditions. Precipitation or dissolution reactions in the alloy samples give rise to heat evolution or absorption, the time derivative of which is depicted in the thermograms, normalized to the specimen mass. The particular reactions appear as peaks in the thermograms. The area of the reaction peak is proportional to the reaction heat (reaction enthalpy).

For the electron microscopy investigations thin foils were prepared by the ordinary electrolytic jet polishing technique with a mixture of methanol and HNO_3 (2:1) at 253 K, 10 V. Using a JEOL 200 CX transmission electron microscope equipped with a top entry specimen holder the specimens could be observed with an ultra high resolution. The spherical aberration coefficient of the objective lens, C_S, was 1 mm. By tilting to a low index zone axis and carefully adjusting the astigmatism the lattice fringes of aluminium as well as the Al_3Li-particles could be imaged.

3 Results

3.1 Calorimetric Investigations

The DSC thermograms of two specimens artificially aged at 433 K for 10 h and at 473 K for 16 h, respectively, are shown in Fig. 1. The samples were solution heat treated for 30 min at 838 K, water-quenched and aged at RT for about 100 h prior to artificial ageing. Both thermograms display two endothermal peaks indicating dissolution processes in the samples. The peak temperature of the significantly larger main peaks are 515 and 552 K after the 433 K and the 473 K ageing, respectively. In accordance with the results of previous investigations[13) 10 15)] this endotherm reaction is attributed to the dissolution of δ' precipitates formed during the artificial ageing. This peak is larger after the 433 K heat treatment where as a consequence of the higher supersaturation a larger amount of the δ' phase is formed than at 473 K. The heat of dissolution of the δ' precipitates was determined from the area of the peak and was found to be 19 J g^{-1} for the 433 K ageing and 14.3 J g^{-1} for the 473 K ageing.

The pre-peaks in the two thermograms of Fig. 1 indicate a reaction at temperatures below the temperature of artificial ageing. Obviously the pre-peaks reflect the dissolution of precipitates formed at RT during the rather long time period between the artificial ageing treatment and the calorimetric measurement. This assumption is confirmed in Fig. 2 by the DSC curves which were taken after different times of natural ageing at RT subsequent to the 433 K and

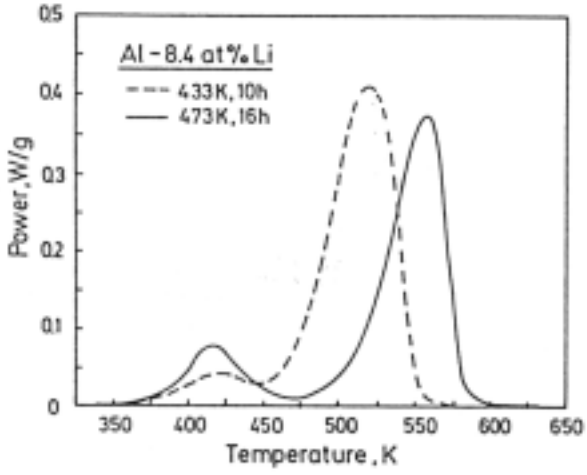

Fig. 1. DSC thermograms of two Al-8.4 at.% Li samples stored at RT for 3 months subsequent to the artificial ageing.

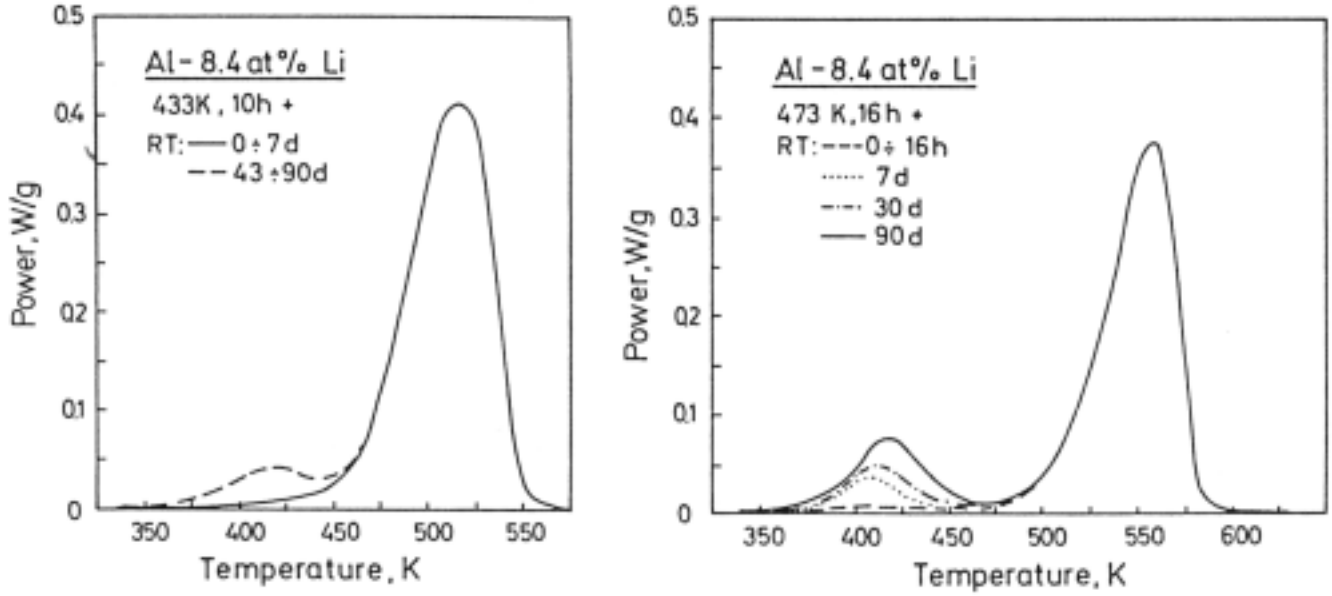

Fig. 2. 2a and b. DSC curves after different times of RT post-ageing following (a) 433 K, 10 h and (b) 473 K, 16 h artificial ageing.

473 K artificial ageing treatments. It is clear that the pre-peak increases with increasing time of RT post-ageing, while the main peak reflecting the dissolution of δ' precipitates formed during artificial ageing remains unchanged. It should be noticed that a very long incubation period preceeds the appearance of the pre-peak, the incubation time runs up to more than 1 week after the 433 K and between 1 and 7 days after the 473 K ageing. The peak temperature of the pre-peak after long-term RT ageing is at about 420 K independent of the artificial ageing temperature. In Fig. 2b it can be seen that with increasing time at RT both the area and the peak temperature of the prepeak are increasing. The reaction heat corresponding to the pre-peak after the longest RT ageings investigated was found to be 2.8 J g^{-1} in the case of the 473 K and 1.5 J g^{-1} after the 433 K ageing treatment. The determination of both reaction heats is of course much more uncertain than that of the main peaks since the overlapping with the main peak gives rise to a large relative inaccuracy, especially in the case of the 433 K ageing.

We have determined the heat of dissolution of the δ' precipitates formed during different artificial ageing treatments between 403 and 473 K in a series of different composition Al-Li alloys. In Table 1, the composition of the alloys, the applied heat treatments, the heat of dissolution (ΔH) and the volume fraction of δ' precipitates, f, are given. The latter was calculated by the equation

$$f = \frac{X - X_\infty}{X_p - X_\infty} \qquad (1)$$

where X is the Li concentration in the alloy, X_∞ and X_p are the Li concentrations in metastable equilibrium at the ageing temperature in the solid solution matrix and in the precipitates, respectively. The values X_∞ and X_p were taken from the metastable miscibility gap determined by Cocco, Fagherazzi and Schiffini[16]. The difference in the specific volume of the solid solution and the δ' phase is very small[17][18] and was neglected in Eq. (1). The heat of dissolution of the δ' phase is plotted against its volume fraction in Fig. 3. It can be seen that within the experimental error bars the points are situated along a straight line from the slope of which (1.35 ± 0.15) J g^{-1}/vol.% is obtained for the heat of dissolution of δ' precipitates. The fact that a straight line was obtained (Fig. 3) confirms that at the different ageing times and temperatures the metastable equilibrium had been attained.

Table 1. The volume fraction, f, as calculated from the metastable miscibility gap[16]) and the heat of dissolution, ΔH, of δ' precipitates in different Al-Li alloys after different ageing treatments.

C_{Li} (at.%)	Heat treatment	f (vol.%)	ΔH(J/g)
6.87	403 K/16 to 90 h	7.3	10.4
6.70	433 K/16 to 40 h	3.8	5.1
8.40	433 K/10 h	14.1	19.0
8.80	433 K/10 h	16.3	22
9.34	433 K/10 h	19.5	27
10.9	433 K/10 h	28.6	35
11.4	433 K/10 h	31.8	47
8.4	473 K/16 h	11.7	14.3
8.6	473 K/48 h	13.0	17.3

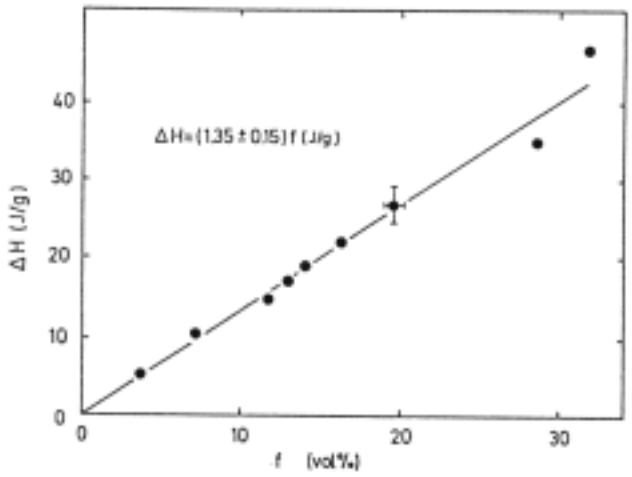

Fig. 3. Heat of dissolution of δ' precipitates formed in course of different artificial ageing treatments vs. volume fraction of the precipitates. (See text and Table 1 for more details.)

3.2 Electron Microscopy

On the basis of the calorimetric results the samples were expected to contain two sets of precipitates of different

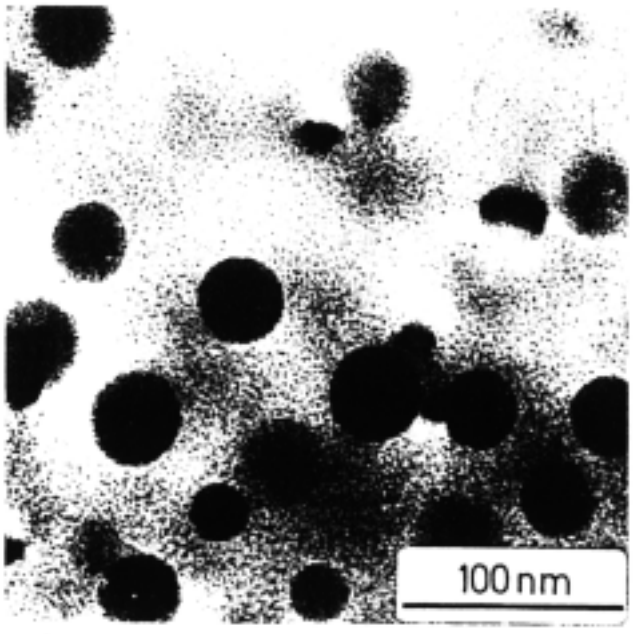

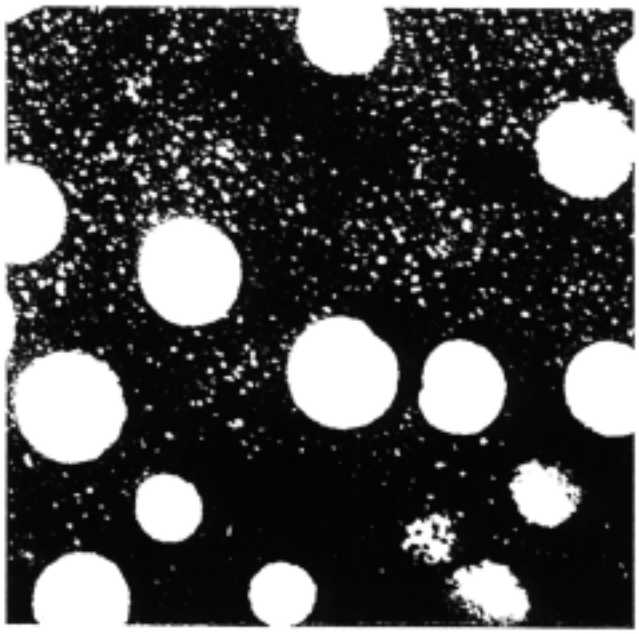

Fig. 4a and b. Bright field (a) and dark field (b) micrograph of an Al-8.6 at.% Li specimen stored for 3 months at RT following 48 h ageing at 433 K

thermal stability. This assumption has been verified by electron microscopy investigations. Fig. 4a shows a bright field micrograph of an Al-8.6 at.% Li specimen solution heat treated, quenched into water, naturally aged for 100 h at RT, aged at 473 K for 48 h and stored at RT for 3 months thereafter. In this micrograph Al_3Li particles of about 40 nm in diameter can be seen as dark spots. The micrograph in Fig. 4b shows the same area taken with the (110) superlattice reflection of the δ' (Al_3Li) phase (dark field image). Beside the larger (about 40 nm mean diameter) δ' particles a very large number of small spots can be seen arising from particles of a few nanometers in diameter.

In the HREM micrograph of the same specimen (Fig. 5) the [111] lattice planes of the aluminium matrix are imaged by tilting to a [110] zone axis. Both the larger and the smaller precipitates are clearly visible in the micrograph. Within the precipitates the (001) and the (110) lattice planes can be seen as indicated in Fig. 6 showing the same area in higher magnification. The change in contrast is caused by the superstructure reflexions (001) and (110).

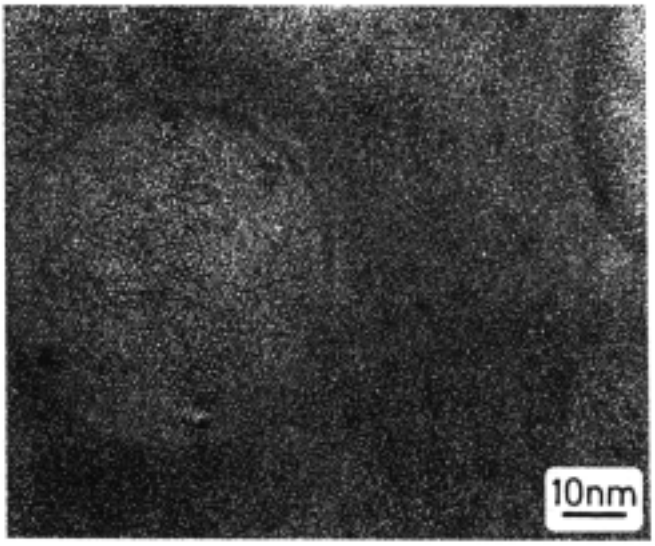

Fig. 5. HREM micrograph of the same specimen as in Figure 4.

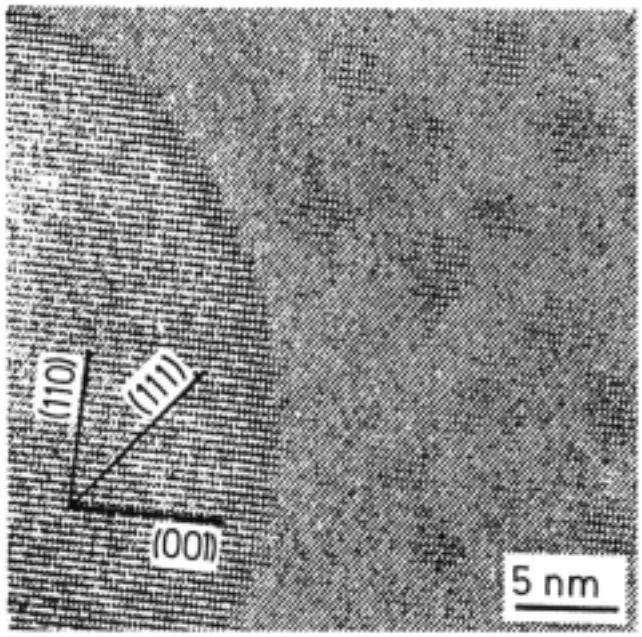

Fig. 6. Lattice image showing the same area of the specimen as Fig. 5 in higher magnification.

The average size of the larger particles is about 40 nm, that of the smaller ones about 4 nm. The particle/matrix interface of the larger δ' particles is very sharp and well defined in contrast to the interfaces of the small particles which seem to be less defined. It has to be mentioned, however, that the imaging conditions are not optimal for the small particles since the thickness of the foil is much larger than the diameter of the small precipitates and, therefore, the scattering of the electrons is also strongly influenced by the matrix. Nevertheless, it can be established beyond any doubt that the atomic arrangement within the small precipitates is very similar to the ordered $L1_2$ structure of the larger δ' particles.

The size distribution of the precipitates has been determined quantitatively by using an image analysing system. A 1 · 1 μm^2 area was selected from the micrograph in Fig. 4b, which contained 152 large and about 20000 small precipitates. The maximum value of the particle radii in the investigated area was determined to be 35.0 nm. The interval from 0 to 35 nm was subdivided into 20 equidistant classes and the number of particles with radii falling in the different classes has been counted. In the case of the

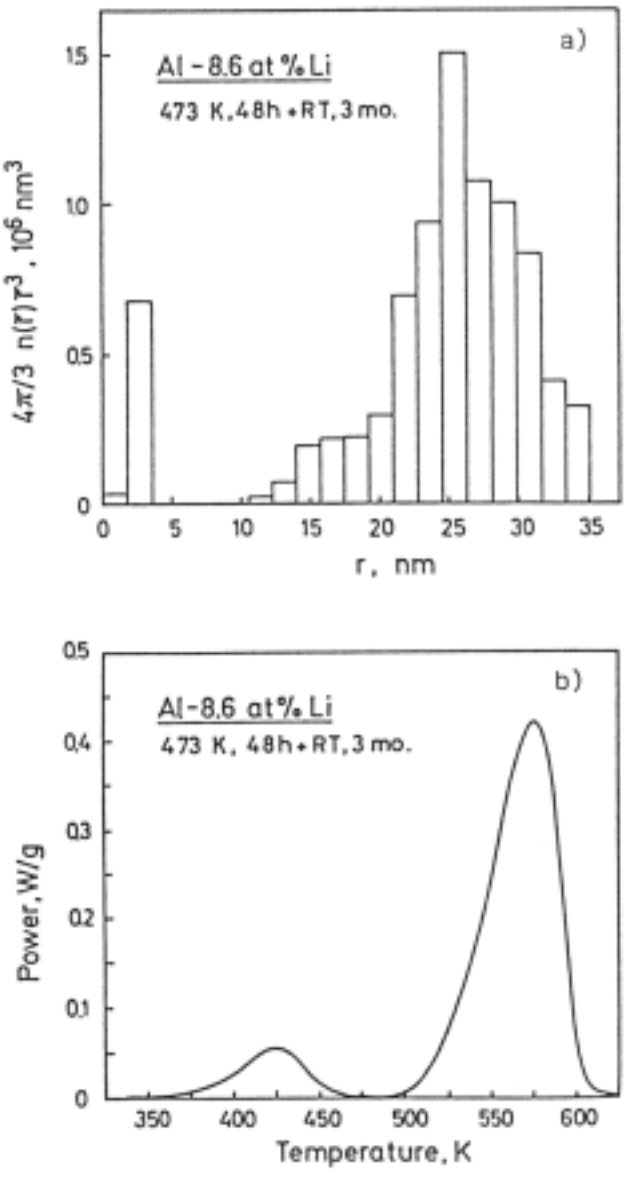

Fig. 7a and b. Volume distribution of precipitates exhibiting (a) the bimodal size-distribution and (b) the corresponding DSC thermogram.

larger particles all the 152 precipitates have been evaluated, while in the case of the small ones only 200 particles were measured and the results of these counts were multiplied by 100 to reach the sum of 20000 in the investigated area. Thereafter, the volume of precipitates in each class was determined as $4\pi\, n(\bar{r})\bar{r}^3/3$, where $n(\bar{r})$ is the number of particles in the corresponding class. This volume distribution is shown in Fig. 7a. The DSC curve of the same specimen can be seen in Fig. 7b, where the dissolution of both the small and the larger particles is demonstrated by the lower left-hand and the higher right-hand peak, respectively.

From the volume distribution in Fig. 7a it can be seen that there is no overlapping in the bimodal particle size distribution. The radii of the RT particles were found to fall between 1.06 and 3.13 nm, while those of the larger δ' precipitates between 7.6 and 35 nm. The mean radius of the small particles was 1.77 nm, that of the large ones 22.0 nm. The total volume of small particles is more than 11 times smaller than that of the large precipitates, their number density, on the other hand is by at least 130 times higher than that of the large ones.

4 Discussion

The decomposition processes in dilute binary Al-Li (6–14 at.% Li) alloys have already been studied by many workers and the sequence

$$\text{supersaturated solid solution} \rightarrow \delta'(Al_3Li) \rightarrow \delta(AlLi),$$

originally proposed by Silcock[19]) is generally accepted[1)2)3]). The δ' phase is formed by homogeneous precipitation from the supersaturated solid solution and it is generally believed that this phase precipitates already during the quenching or after it, even in the temperature range around RT[15]) to 25]). There are a few investigations, however, in which a second level of metastability whithin the $\alpha + \delta'$ phase field is proposed and interpreted in terms of GP zone formation at temperatures near RT[13)26]) to 28]). Except the theoretical work of Sigli and Sanchez based on the cluster variation method[27]), all these investigations are based on calorimetric measurements which – similarly to our DSC results – display an extra dissolution peak besides the peak attributed to the dissolution of the δ' precipitates. Our TEM and HREM results, on the other hand, demonstrate that at RT particles of the same ordered $L1_2$ structure as that of the δ' precipitates are formed. Their average size, however, is considerably smaller and the particle/matrix interface seems to be not so well defined than that of the δ' particles formed in the temperature range between 433 and 473 K. In consequence of this structural identity we will not postulate, like some other authors, the existence of GP zones in the Al-Li alloys investigated here. This problem will be discussed later on in more detail.

The results of our DSC and electron microscopy investigations show that in Al-Li alloys artificially aged at 433 or 473 K further nucleation of δ' particles takes place during the RT storage following the artificial ageing treatment. After long-term RT post-ageing TEM and HREM micrographs reveal a bimodal distribution of δ' precipitates in the samples with considerably different mean particle sizes. The reason for this post-ageing phenomenon is the significantly different solubility of Li in Al at 433 to 473 K and at RT, respectively. According to the metastable miscibility gap determined by Cocco et al.[16]) the solute Li concentration in equilibrium with the metastable δ' phase is 6.6 at.% at 473 K, 6.1 at.% at 433 K and 5.0 at.% at RT, respectively. This means that the concentration of solute Li atoms is decreased by δ' precipitation to 6.1 at.% during the heat treatment at 433 and to 6.6 at.% at 473 K. If the sample is transferred to RT thereafter, the solid solution becomes supersaturated again and consequently further precipitation sets in as confirmed by HREM. The fact that this precipitation takes place by the formation of new particles instead of further growth of the already existing large δ' particles indicates that no significant nucleation difficulty is involved in the formation of the precipitates. This is consistent with the small particle/matrix interface energy and misfit strain energy in the case of the fully coherent δ' precipitates[22]).

The specific interface energy, γ, of the δ' particles formed at 473 K has been determined by Baumann and Williams[21]) to be 14 mJ m^{-2} on the basis of the capillarity (Gibbs-Thompson) equation,

$$X_r = X_\infty \exp\left\{\left(\frac{1 - X_\infty}{X_p - X_\infty}\right) \cdot \left(\frac{2\gamma V_m}{r R_g T}\right)\right\} \qquad (2)$$

where X_r and X_∞ are the concentration of solute in the matrix at interfaces of particles with radius r and infinity (∞), respectively. The quantity X_p represents the concentration of solute in the precipitate phase, V_m is the molar volume and R_gT is the thermal energy. The maximum value of X_r in Eq. (2) is of course the average concentration of the matrix, defining thereby a minimum size of r, which is the size of the critical nucleus, r_{cr}. Taking the above value for γ and X_∞ = 5 at.%, X_p = 24.6 at.% for the miscibility gap at RT[16]) with $V_m = 10^{-5}$ m^3, the critical nucleus size, r_{cr} for the RT particles, can easily be calculated from Eq. (2). After the 473 K ageing (solute concentration in the matrix 6.6 at.%) r_{cr} = 1.9 nm, while after the 433 K ageing (matrix concentration 6.1 at.%) r_{cr} = 2.7 nm is obtained. These r_{cr} values are too large taking into account that the radius of the smallest particles observed after long-term RT ageing is about 1 nm following ageing at 473 K. Taking this value as r_{cr} Eq. (2) would be valid if the solubility limit X_∞ at RT would be reduced from 5 to approximately 4 at.%. Since this value would be within the limits of accuracy the size of the critical nucleus could be explained this way.

Another possibility is a reduced specific interface energy of the RT particles. Our HREM micrographs show very sharp, well defined, interfaces in the case of the large δ' particles formed during the artificial ageing and rather diffuse interfaces in the case of the precipitates formed at RT. The smaller specific interface energy of the RT particles may be caused by their nearly stoichiometric composition and a higher amount of structural defects in the particles. On the basis of the HREM micrographs the critical nucleus size at RT is certainly not larger than 1 nm after the 473 K ageing, correspondingly the specific interface energy of the RT particles may not be larger than 10 mJ m^{-2}.

The DSC measurements indicate a rather long incubation time at RT before the appearance of the pre-peak (Fig. 2). The solute concentration in the matrix decreases to 6.6 at.% Li during the artificial ageing at 473 K. Ceresara et al.[20]) have investigated by resistometric method the precipitation processes among others in an Al-Li alloy of practically the same concentration (Al-6.67 at.% Li) and they observed no detectable incubation period upon ageing at or near RT after quenching the alloy from 623 K, the formation of the ordered precipitates could be clearly detected already within the first minute after quenching. The reason

for this difference is probably the higher vacancy concentration after quenching from 623 K.

We have other indirect indications for the important role of the excess vacancies in the RT ageing process as well. Taking into account the fully coherent nature and the spherical shape of the particles it can be expected that the size of the RT precipitates increases according to bulk diffusion controlled kinetics. In this case the particle radius r will increase parabolically with time t:

$$r = \lambda(Dt)^{1/2} \tag{3}$$

where λ is a function of the supersaturation[29]) and D the diffusion coefficient. For the case of the RT post-ageing using again the data from Cocco et al.[16]) for the determination of the supersaturation the value of λ is 0.5 after the 473 K ageing. Taking the average value of r on the basis of the HREM investigations as 1.7 nm after 3 months of ageing we can estimate an effective diffusion coefficient for the RT ageing process as about $1.7 \cdot 10^{-24}$ m^2 s^{-1}. The value of D extrapolated from the high temperature measurements of Costas[30]) as well as the data from the kinetic investigations of Jensrud and Ryum[31]) near 473 K would yield a diffusion coefficient of the order of 10^{-28} m^2 s^{-1} for RT. This discrepancy of 4 orders of magnitude can only be explained by supposing that at RT vacancies frozen in from the temperature of the artificial ageing treatment enhance the diffusion process for a rather long period of time. The binding energy between a vacancy and a Li atom has been determined by Ceresara et al.[20]) to be 0.25 ± 0.03 eV. On the basis of this high vacancy – Li binding energy the growth kinetics of the δ' particles at 473 K has also been interpreted by Baumann and Williams[22]) by supposing that most of the vacancies are bound to Li atoms. Accepting this assumption the factor 10^4 between the diffusivity estimated from our experiments and that extrapolated from the equilibrium measurements would be consistent with a 0.61 eV effective formation energy of vacancies in the alloy. This value, although smaller than the 0.76 eV generally accepted for pure aluminium, is considerably larger than the 0.51 eV formation energy reported by Ceresara et al.[20]), consequently the binding energy between Li atoms and vacancies should be somewhat smaller, about 0.15 eV.

On the basis of calorimetric measurements the heat of dissolution of δ' precipitates formed at different temperatures between 403 and 473 K was calculated to be 1.35 ± 0.15 Jg^{-1}/vol.%. Accepting this value also for the precipitates formed at RT, from the reaction heat in the pre-peaks in Fig. 2 (2.8 J/g after 473 K and 1.5 J/g after 433 K ageing) the volume fraction of the RT particles after long-term RT ageing should be about 2 and 1 vol.% after the 473 and 433 K ageing, respectively, in the Al-8.4 at.% Li alloy. Similarly from the thermogram in Fig. 7b the volume fraction of the RT precipitates in the Al-8.6 at.% Li alloy should be about 1.5 %. It should be noted that in this way the volume fraction of the RT particles might be underestimated since their heat of dissolution might be somewhat smaller than that of the high temperature δ' precipitates in consequence of the higher concentration of structural defects in the small particles. From the volume distribution in Fig. 7a for the same alloy it was shown that the volume fraction of the RT precipitates is 11 times smaller than that of the 473 K precipitates. So, accepting the 13 % volume fraction value from Table 1 for the 473 K δ' particles calculated from the metastable miscibility gap, a volume fraction of 1.2 % is obtained for the RT precipitates, which is close to the value obtained from the calorimetric measurement. It should be mentioned that the volume of the smaller precipitates might be somewhat underestimated in the quantitative TEM analysis as well, since the TEM foils are by one order of magnitude thicker than the average size of the small particles, which probably causes overlapping of small particles in the micrograph.

In the case of the small particles formed at RT it might be possible that the contribution of the particle/matrix interface energy must be taken into consideration. For spherical precipitates this contribution can be easily calculated:

$$E_s = \frac{3f\gamma}{\rho r} \tag{4}$$

where f is the volume fraction, γ the specific interface energy, r the average radius of the precipitates and ρ the density of the alloy. Taking $\rho = 2500$ kg/m^3, $r = 1.77$ nm, an interface contribution of only 0.1 Jg^{-1}/vol.% is obtained. This contribution is smaller than the experimental error in the determination of the heat of dissolution from the pre-peak in the thermograms and can be accordingly neglected. So it can be established that the volume fraction of the precipitates formed during the RT post-ageing is about 1.5 vol.% in the 8.6 at.% Li alloy after 473 K artificial ageing treatment.

The amount of the RT particles decreases with increasing Li concentration in the alloy and with decreasing artificial ageing temperature. This can be seen if the volume fraction of the RT particles is calculated from the data of the metastable miscibility gap:

$$f_2(\delta') = \left(\frac{X_{1p} - X}{X_{1p} - X_{1\infty}}\right) \cdot \left(\frac{X_{1\infty} - X_{2\infty}}{X_{2p} - X_{2\infty}}\right) \tag{5}$$

where $X_{1\infty}$ and X_{1p} are the atomic concentrations of Li in metastable equilibrium at the first (higher) ageing temperature in the solid solution matrix and in the precipitates, respectively. $X_{2\infty}$ and X_{2p} are the same quantities for the second ageing temperature (RT in this case), and X is the bulk concentration in the alloy. Equation (5) takes into account that the precipitation at the second ageing temperature takes place only in that part of the whole sample which has not been occupied by δ' precipitates during the first ageing. Here, for the same reasons as in the case of Eq. (1), the differences in the specific volumes are neglected.

Using again the data of Cocco et al.[16]) ($X_{1\infty}$ = 6.6 resp. 6.1 at.%, X_{1p} = 22 resp. 23 at.% for the 473 resp. 433 K ageing and $X_{2\infty}$ = 5.0 and X_{2p} = 24.6 at.% for the RT post-ageing) the volume fraction of the precipitates formed during the RT ageing was calculated from Eq. (5) with X = 8.6 at.% to be 7.1 resp. 4.2 vol.% following the 473 resp. 433 K ageing. It can be seen that the calculated volume fractions are by at least a factor of 4 higher than the values obtained from the experimental results. This large difference can be explained, however, if the small size of the RT particles is taken into account which increases the concentration of Li atoms retained in solid solution from around 5 at.% to larger values of 6 at.% or even higher. For example, a volume fraction f_2 = 1.4 % is obtained using the following set of data in accordance with Eq. (2) : γ = 10 mJ m^{-2}, r = 1.77 nm, $X_t = X_{2\infty}$ = 6.3 %, $X_{1\infty}$ = 6.6 %, X_{1p} = 22 % and X_{2p} = 24.6 %. This shows that the metastable equilibrium at RT is not reached even after several months of post-ageing.

Now the question of the existence of GP zones in Al-Li alloys can be discussed. If by GP zones fully coherent metastable precipitates are meant, then the δ' precipitates might alternatively be called GP zones as well, as it

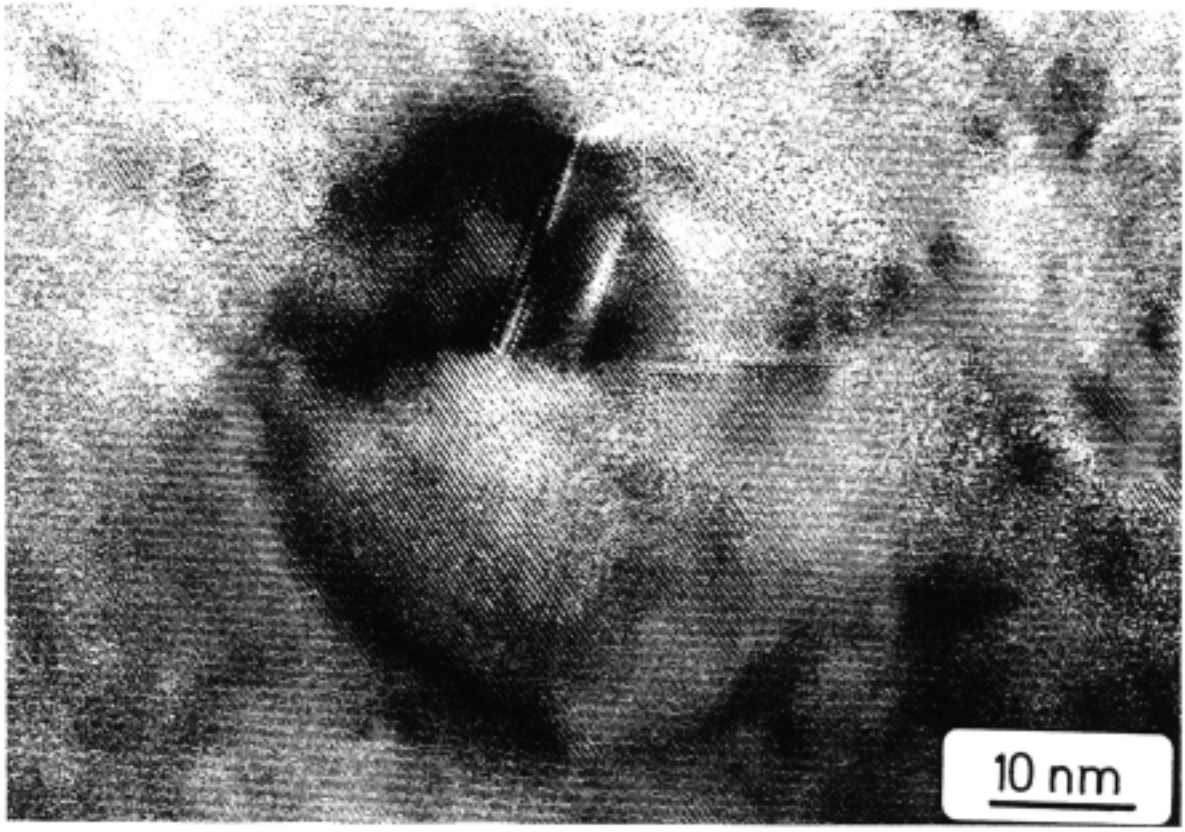

Fig. 8. HREM micrograph of a cyclically deformed specimen showing super dislocations shearing a δ' particle of about 30 nm diameter.

was done in the papers of Ceresara et al.[20][32]) and Cocco et al.[16]). In these works, however, δ' and GP zones denote the same precipitates. Another example, where $L1_2$ ordered particles of a well defined stoichiometry are termed GP zones are the Al_3Mg particles in Al-base Al-Mg alloys[33]). It is more common, however, to use some other denotation for precipitate phases with well defined and known structure and composition, like e.g. γ' precipitates in the Fe- and Ni-base superalloys. In this sense – although it seems to be more adequate to term the coherent $L1_2$ ordered Al_3Li precipitates as δ' – it is only a question of terminology.

A problem which is of much more relevance would be whether to postulate in Al-Li alloys the existence of GP zones which are distinct from δ' precipitates, emphasizing thereby the existence of another kind of precipitate which is structurally and/or compositionally different from the δ' phase as it has been proposed on the basis of theoretical model calculations[27]) and of calorimetric investigations[13][26][28]). The present investigations clearly show that there is no relevant structural difference between the precipitates formed at RT and those formed in the temperature range of 403 to 473 K. The work of Cocco et al.[16]) demonstrates that the average composition of the RT particles corresponds to the same Al_3Li stoichiometry as that of the δ' particles. The present DSC results in combination with electron microscopy, as discussed above, show no significant difference in the heat of dissolution/vol.% of the particles formed at RT and those formed at temperatures between 130 and 473 K. The only differences are in the size and in the quality of the particle/matrix interface and a probably higher defect concentration in the small particles. These differences, however, in the authors' opinion do not require the introduction of a GP zone phase which would be physically different from the δ' phase.

HREM investigations have been undertaken also on Al-8.6 at.% Li samples which were only naturally aged at RT for about 6 weeks after quenching from 803 K. The precipitates in this sample have the same characteristics as the particles formed during the RT ageing subsequent to artificial ageing treatment. Similar observations were also made by HREM investigations by Sato et al.[34]). Therefore, it is the authors' belief that the decomposition of the supersaturated solid solution in Al-Li alloys of compositions between about 5 and 14 at.% in the temperature range from RT to 473 K takes place by the formation of metastable δ' precipitates and there is no physical reason to postulate another level of metastability, i.e. the existence of GP zones in this system.

The RT storage after the artificial ageing of Al-Li alloys is leading to a bimodal distribution of δ' precipitates with two significantly different mean sizes. Consequently, the dissolution of the precipitates takes place in different temperature regions if the temperature is continously increased as in the DSC measurements. The smaller and the larger particles show different behaviour in the course of plastic deformation as well[35]) although even the larger δ' particles (up to about 50 nm diameter) become sheared by dislocations as it is demonstrated by the HREM micrograph of a cyclically deformed specimen in Fig. 8. It can be seen that in the δ' particle of about 30 nm diameter in the direction of the (111) lattice planes the lattice image is disturbed by super dislocations shearing the particle. The strength and the deformation characteristics of artificially aged alloys are mainly determined by the ensemble of larger particles[8]) but also solely the RT particles lead to – however limited – strengthening and strain localization in samples aged only at RT after quenching. More detailed investigations on the mechanical properties of the samples will be published in a subsequent paper.

5 Conclusions

1. During the RT storage of Al-Li alloys aged previously for 10 to 50 h at 433 to 473 K further precipitation takes place by the formation of small new particles after a rather long incubation period. This second ageing leads to a bimodal distribution of precipitates with strongly differing mean particle sizes.

2. The occurrence of the RT post-ageing phenomenon could be explained on the basis of the $\alpha + \delta'$ metastable miscibility gap since with cooling to RT the depleted matrix becomes supersaturated again. Because of the smallness of the particles only a small volume fraction of the order of 1 to 2 vol.% can precipitate which is much less than expected from the equilibrium conditions of the metastable miscibility gap. This means that the matrix remains supersaturated according to the Gibbs-Thompson equation.

3. The kinetics of the RT post-ageing indicates a diffusivity which is about 4 orders of magnitude higher than that corresponding to the equilibrium diffusion coefficient. This diffusivity is a consequence of the vacancies frozen in from 473 K. A strong vacancy-Li binding hinders them from fast annealing-out, although the binding energy seems to be somewhat smaller than the 0.25 eV value reported in the literature.

4. The precipitates formed at RT contain probably a higher amount of crystal defects, have a lower specific interface energy but have the same ordered $L1_2$ structure and the same stoichiometry as the δ' precipitates formed during artificial ageing at temperatures between 433 and 473 K.

5. The precipitates formed at or near RT in dilute Al-Li alloys are δ' particles and there is no physical reason to postulate the existence of a GP zone phase which is different from the δ' phase as it has been proposed in some cases in the literature.

The authors are grateful to Prof. W. Gust for a valuable discussion on interface energies and nucleation of precipitates. One of the authors, J. L., gratefully acknowledges support by the Max-Planck-Gesellschaft for a stay at the Max-Planck-Institut für Metallforschung, Stuttgart.

Literature

[1] D. B. WILLIAMS, in Aluminium-Lithium, T. H. Sanders, Jr., E. A. Starke, Jr. (eds.), TMS-AIME (1981) 89.
[2] T. H. SANDERS, Jr. and E. A. STARKE, Jr., in Aluminium-Lithium II, E. A. Starke, Jr., T. H. Sanders, Jr. (eds.), TMS-AIME (1984) 1.
[3] W. LACOM, Mater. Sci. Forum **13/14** (1987) 69–84.
[4] Y. MIURA, A. MATSUI, M. FURUKAWA, and M. NEMOTO, Aluminium-Lithium Alloys III, C. Baker, P. J. Gregson, S. J. Harris, C. J. Peel (eds.), The Institute of Metals, London (1986) 427–434.
[5] Y. MIURA, K. YUSU, M. FURUKAWA, and M. NEMOTO, J. de Physique, Colloque C3, supplément au n° 9, **48** (1987) C3-549-555.
[6] M. FURUKAWA, Y. MIURA, and M. NEMOTO, Trans. JIM **26** (1985) 230–235.
[7] M. FURUKAWA, Y. MIURA, and M. NEMOTO, Trans. JIM **27** (1986) 14–22.
[8] J. SCHNEIDER, H.-J. GUDLADT, and V. GEROLD, J. de Physique, Colloque C3, supplément au n° 9, **48** (1987) C3-745-751.
[9] B. LERCH and V. GEROLD, Acta metall. **33** (1985) 1709–1716.
[10] J. GLAZER, and J. W. MORRIS, Jr., Phil. Mag. A **56** (1987) 507–515.
[11] Th. STEFFENS, Ch. SCHWINK, A. KORNER, and H.-P. KARNTHALER, Phil. Mag. A **56** (1987) 161–173.
[12] H.-P. KARNTHALER and B. SCHÜGERL, Strength of Metals and Alloys, P. Haasen, V. Gerold and G. Kostorz (eds.), Pergamon Press, Oxford (1979) 205–210.
[13] J. M. PAPAZIAN, C. SIGLI, and J. M. SANCHEZ, Scripta metall. **20** (1986) 201–206.
[14] J. M. PAPAZIAN, G. G. BOTT, and P. SHAW, J. de Physique, Colloque C3, supplément au n° 9, **48** (1967) C3-231-237.
[15] F. LIVET and Y. BRECHET, J. de Physique, Colloque C3, supplément au n° 9, **48** (1987) C3-357-362.
[16] G. COCCO, G. FAGHERAZZI, and L. SCHIFFINI, J. Appl. **10** (1977) 325–327.
[17] B. NOBLE and G. E. THOMPSON, Metal. Sci. J. **5** (1971) 114–120.
[18] D. B. WILLIAMS, and J. W. EDINGTON, Metal Science **9** (1975) 529–532.
[19] J. M. SILCOCK, J. Inst. Metals **88** (1959/60) 357–364.
[20] S. CERESARA, A. GIARDA, and A. SANCHEZ, Phil. Mag. **35** (1977) 97–110.
[21] S. F. BAUMANN and D. B. WILLIAMS, Scripta metall. **18** (1984) 611–616.
[22] S. F. BAUMANN and D. B. WILLIAMS, Metall. Trans. **16A** (1985) 1203–1211.
[23] F. LIVET and D. BLOCH, Scripta metall. **10** (1985) 1147–1151.
[24] J. M. GENTZBITTEL, G. VIGIER, and R. FOUGERES, J. de Physique, Colloque C3, supplément au n° 9, **48** (1987) C3-729-735.
[25] A. G. KHACHATURYAN, T. F. LINDSEY, and J. W. MORRIS, Jr., Metall. Trans. **19A** (1988) 249–258.
[26] R. NOZATO and G. NAKAI, TRANS JIM **18** (1977) 679–689.
[27] C. SIGLI and J. M. SANCHEZ, Acta metall. **34** (1986) 1021–1028.
[28] A. K. MUKHOPADHYAG, C. N. J. TITE, H. M. FLOWER, P. J. GREGSON, and F. SALE, J. de Physique, Colloque C3, supplément au n° 9, **48** (1987) C3-439-446.
[29] H. B. AARON, D. FAINSTEIN, and G. R. KOTLER, J. Appl. Phys **41** (1970) 4404-4410.
[30] L. P. COSTAS, USAEC Report DP-813 (1983).
[31] O. JENSRUD and N. RYUM, Mater. Sci. Eng. **64** (1984) 229–236.
[32] S. CERESARA, G. COCCO, G. FAGHERAZZI, and L. SCHIFFINI, Phil. Mag. **35** (1977) 373–378.
[33] A. DAUGER, M. FUMERON, and J. P. GUILLOT, J. Appl. Cryst. **12** (1979) 429–431.
[34] T. SATO, N. TANAKA, and T. TAKAHASHI, Trans. JIM **29** (1988) 17–25.
[35] J. LENDVAI, H.-J. GUDLADT, and V. GEROLD, Scripta metall. **22** (1988) 1755–1760.

(Eingegangen am 8. Dezember 1988)